A MULTIPOLE MODEL FOR $K\Sigma$ PHOTOPRODUCTION IN FOUR ISOSPIN CHANNELS

T. Mart

Departemen Fisika FMIPA, Universitas Indonesia, Depok 16424, Indonesia

QNP 2018

KEK Tsukuba, Japan, November 2018

Contents

- Motivation
- Progress in the $K\Lambda$ photoproduction
- Progress in the $K\Sigma$ photoproduction near threshold
- $K\Sigma$ channels for energies above threshold
- Conclusion

Motivation, Kaon-Maid is getting Old

K

MAID 2000

Institut für Kernphysik, Universität Mainz, Germany

An effective Lagrangian Model for Kaon Photo- and Electroproduction on the Nucleon

T. Mart (University of Indonesia), C. Bennhold and H. Haberzettl (George Washington University), and L. Tiator

References:

For kaon photoproduction:	**F.X. Lee, T. Mart, C. Bennhold, H. Haberzettl, L.E. Wright, Nucl. Phys. A695 (2001) 237, or nucl-th/9907119**
For the missing resonance D_{13}(1900):	**T. Mart, C. Bennhold, Phys. Rev. C61 (2000) 012201, or nucl-th/9906096** **C. Bennhold *et al.*, nucl-th/0008024**
For kaon electroproduction:	**C. Bennhold, H. Haberzettl, T. Mart, nucl-th/9909022**

- **Electromagnetic Multipoles ($E_{l\pm}$, $M_{l\pm}$, $L_{l\pm}$, $S_{l\pm}$)**
- **CGLN and Helicity Amplitudes (F_1,...,F_6, H_1,...,H_6)**
- **Polarized Response Functions (R_T,R_L,R_{LT},R_{TT},$R_{LT'}$,$R_{TT'}$)**
- **Unpolarized 2-fold Diff. Cross Sections (L,T,L,T,TT,LT')**
- **5-fold Diff. Cross Section**
- **Total Cross Sections (T,L,LT,LT',TT')**
- **Transverse Polarization Observables (ds/dW,T,S,P,E,F,...)**
- **Target Polarization (P_x,P_y,P_z)**
- **Recoil Polarization (P_x,P_y,P_z)**

External services:
MAID Homepage MAID2003 MAID2000 DMT2001 ETA-MAID

Other Motivations

1. Elementary operator → isobar model
2. Investigation of the nucleon, kaon, hyperon resonances
3. Study
   - strong coupling constants → $S_{11}(1535)$
   - isospin symmetry
   - strangeness process
4. Gerasimov-Drell-Hearn rum rule
5. Production on deuteron
6. Production of hypernuclei
7. etc (e.g., PDG, job)

Six Possible Isospin Channels

No.	Type	$E_\gamma^{\rm lab.}$ (MeV)	W (MeV)
1)	$\gamma + p \longrightarrow K^+ + \Lambda$	911	1609
2)	$\gamma + n \longrightarrow K^0 + \Lambda$	915	1613
3)	$\gamma + p \longrightarrow K^+ + \Sigma^0$	1046	1686
4)	$\gamma + p \longrightarrow K^0 + \Sigma^+$	1048	1687
5)	$\gamma + n \longrightarrow K^+ + \Sigma^-$	1052	1691
6)	$\gamma + n \longrightarrow K^0 + \Sigma^0$	1051	1690

Intrinsic Problems of the Isobar Model

Problems

- Threshold energies are too high
- Too many nucleon, hyperon, and kaon resonances
  $\rightarrow$ complicated models
- Almost all coupling constants are hardly known
- Higher order corrections are not considered
- Strong couplings are not perturbative!
  $\rightarrow$ Bethe-Salpeter or Lippman-Schwinger equation
  $\rightarrow$ much more complicated

What to do?

- Limit the energy of interest!

$K^+\Lambda$ Photoproduction Near Threshold

The background (non-resonance) terms are constructed from a series of Feynman diagrams as in the previous isobar model (Kaon-Maid)

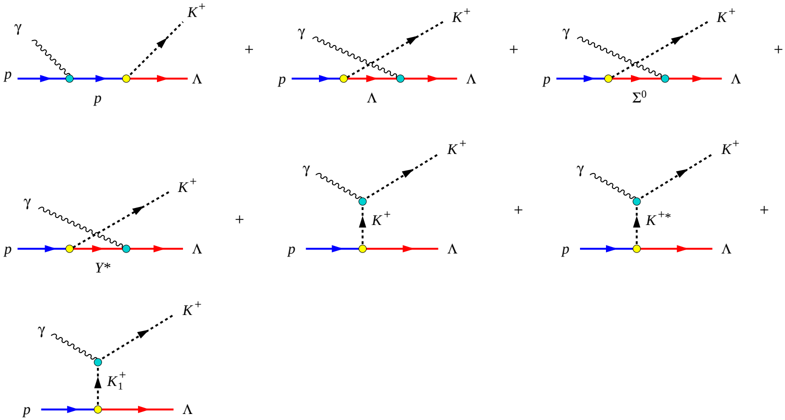

Resonance Term?

For resonance term $S_{11}(1650)$ use multipoles amplitude (Breit-Wigner form):

$$E_{0+}(W) = \bar{E}_{0+}\, c_{K\Lambda}\, \frac{f_{\gamma R}(W)\,\Gamma_{\rm tot}(W) m_R\, f_{KR}(W)}{m_R^2 - W^2 - i m_R \Gamma_{\rm tot}(W)}\, e^{i\phi}$$

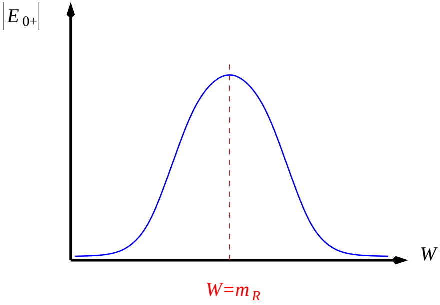

The advantage: Simple and does not generate unnecessary additional background term as in the case of the covariant calculation

see e.g., TM and A. Sulaksono, Phys. Rev. C **74**, 055203 (2006)

Comparison with experimental data

TM, Phys. Rev. C **82**, 025209 (2010)

χPT $\rightarrow$ Steininger and Meissner, Phys. Lett. B **391**, 446 (1997).

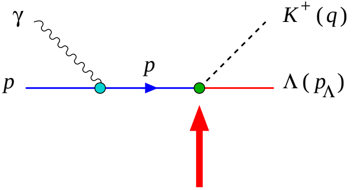

Pseudoscalar (PS): $i\gamma_5 g_{K\Lambda N}$

Pseudovector (PV): $i\gamma_5 \not{q}\, g_{K\Lambda N}$

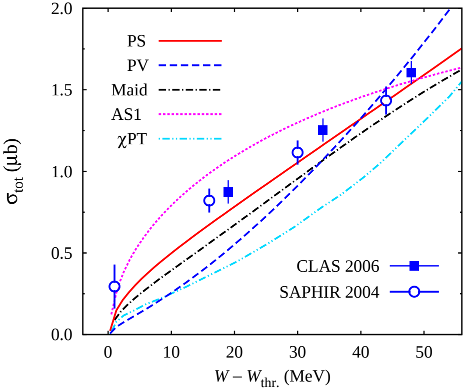

Comparing two theories (PS & PV) with other previous models

PS model can explain better

Comparison with experimental data

Differential cross section [TM, Phys. Rev. C **82**, 025209 (2010)]

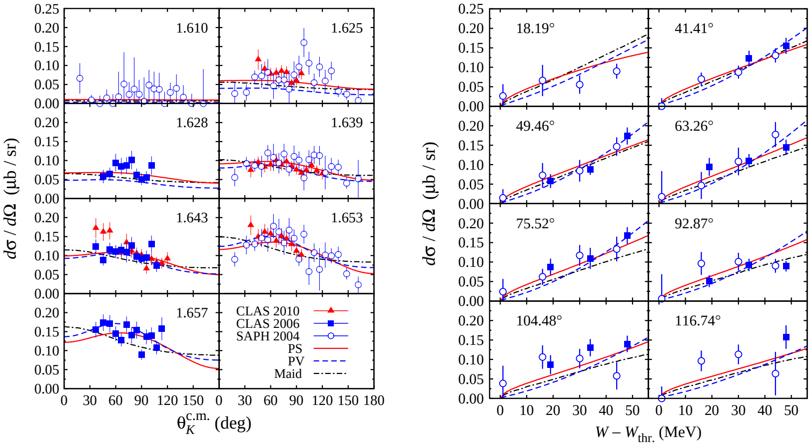

For new result: TM & S. Sakinah Phys. Rev. C **95**, 045205 (2017),
S. Clymton and TM, Phys. Rev. D **96**, 054004 (2017).

$K^0\Lambda$ Photoproduction Near Threshold

No t-Channel K^0 Intermediate State in Photoproduction

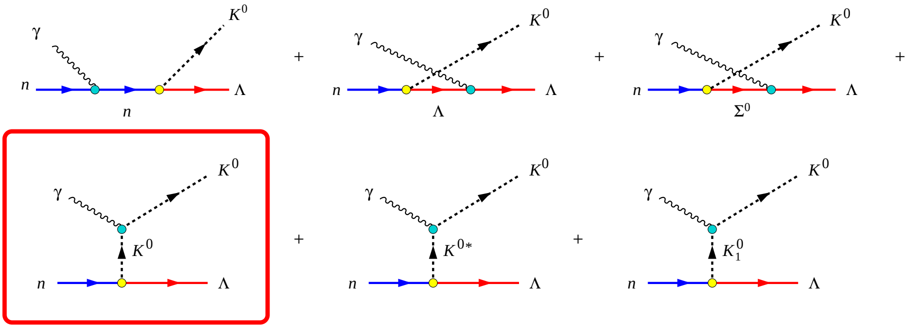

Not allowed except for virtual photons

plus some isospin symmetry relations

Result, predicted total cross section

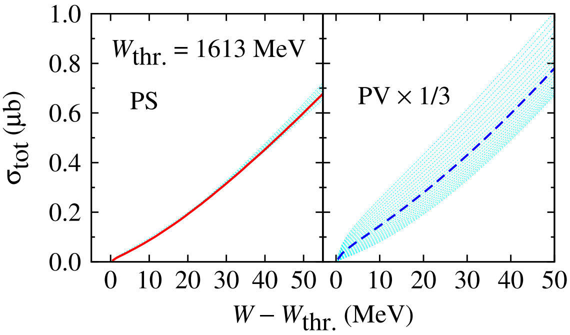

- Significantly smaller than Kaon-Maid prediction
- May affect the predictions made based on Kaon-Maid
- Needs experimental confirmation
  - $\gamma + d \rightarrow K^0 + \Lambda + p$
  - $\gamma + d \rightarrow K^0 + \Sigma^0 + p$

TM, Phys. Rev. C **83**, 048203 (2011)

Extending to $K\Sigma$ Channels

TM, Phys. Rev. C **90**, 065202 (2014).

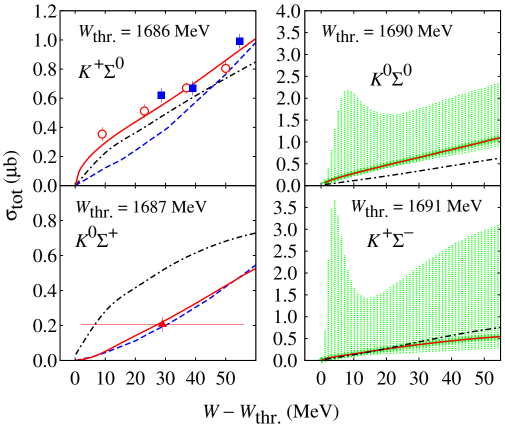

- Cross sections of $K^0\Sigma^0$ and $K^+\Sigma^-$ channels have considerably large uncertainty
- Direct consequence of the uncertainties in the helicity photon couplings $A_{1/2}$ and $A_{3/2}$ taken from PDG
- Needs constraint from $\gamma + d \to K + Y + N$ data

Results for the $K^0\Sigma^+$ Differential Cross Section

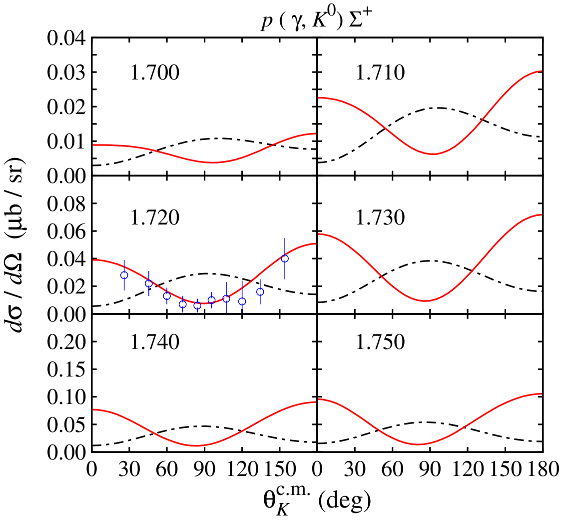

- The agreement with experimental data is okay
- Backward and forward peakings
- TM, Phys. Rev. C **90**, 065202 (2014).

Results for the $K^0\Sigma^+$ Differential Cross Section

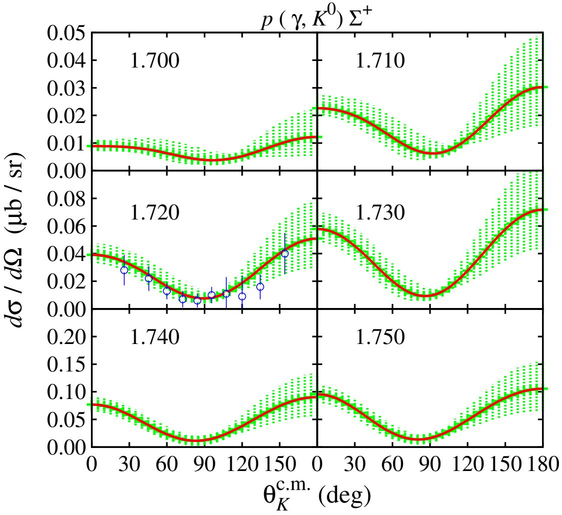

- Depends on the ratio of the $g_{K_1^0 K^0\gamma}/g_{K_1^+ K^+\gamma}$
- Present study: -0.79
- Kaon Maid: -0.45
- Vary by 20%

Results for the $K^+\Sigma^-$ Differential Cross Section

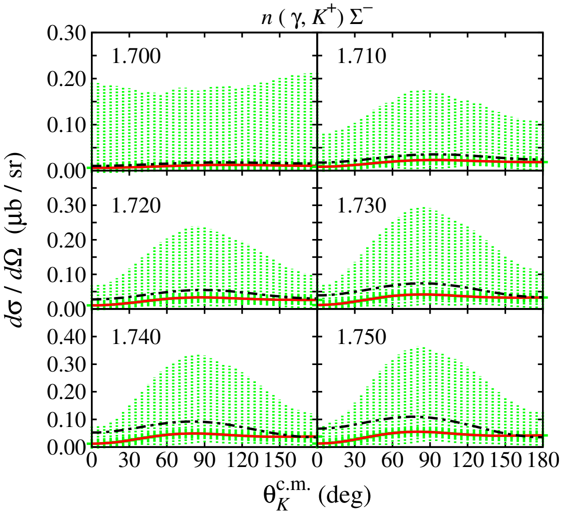

- Uncertainty from helicity photon couplings $A_{1/2}$ and $A_{3/2}$
- Needs information from the γd reactions

$K\Sigma$ channels for energies above threshold

Experimental data used in the present study

Channel	Collaboration	Observable	N
$\gamma + p \to K^+ + \Sigma^0$	SAPHIR 2004	$d\sigma/d\Omega$	480
		P	12
	CLAS 2004	$d\sigma/d\Omega$	676
		P	146
	LEPS 2004	Σ	30
	LEPS 2006	$d\sigma/d\Omega$	39
		Σ	25
	LEPS 2006	$d\sigma/d\Omega$	52
		Σ	26
	CLAS 2006	$d\sigma/d\Omega$	1280
	GRAAL 2007	P	8
		Σ	42
	CLAS 2007	C_x	94
		C_z	94
	CLAS 2010	$d\sigma/d\Omega$	2089
		P	455
	Crystal Ball 2014	$d\sigma/d\Omega$	1129
$\gamma + p \to K^0 + \Sigma^+$	SAPHIR 2005	$d\sigma/d\Omega$	90
		P	10
$\gamma + n \to K^+ + \Sigma^-$	LEPS 2006	$d\sigma/d\Omega$	72
		Σ	36
	CLAS 2010	$d\sigma/d\Omega$	177
Total data			7062

- Kinematics coverage:
  $W = 1.695 - 2.835$ GeV
  $\theta_K \approx 18^\circ - 154^\circ$
- Our goal: fit all data
- Use all nucleon resonances within the covered energies

Nucleon Resonances Used in this Study

Table 2. Properties of the nucleon resonances used in the present work. The helicity amplitudes $A_{1/2}$ and $A_{3/2}$ of both proton and neutron are given in 10^{-3} GeV$^{-1/2}$ units. Data are taken from the Review of Particle Properties of Particle Data Group (PDG).[1]

State	J^P	M_R^a	Γ_R^a	β_K	$A_{1/2}(p)^a$	$A_{3/2}(p)^a$	$A_{1/2}(n)^a$	$A_{3/2}(n)^a$	Overall	Status
$N(1895)S_{11}$	$1/2^-$	1905 ± 12	100^{+30}_{-10}	13 ± 7	12 ± 6	-	3 ± 7	-	**	*
$N(1710)P_{11}$	$1/2^+$	1710 ± 30	150 ± 100	15 ± 10^b	50 ± 10	-	-40 ± 20	-	****	**
$N(1880)P_{11}$	$1/2^+$	1875 ± 40	230 ± 50	17 ± 7	21 ± 6	-	-60 ± 50	-	**	-
$N(2300)P_{11}$	$1/2^+$	$2300^{+40+109}_{-30-0}$	$340 \pm 30^{+110}_{-58}$	-	-	-	-	-	**	-
$N(1720)P_{13}$	$3/2^+$	1720^{+30}_{-20}	250^{+150}_{-100}	$4 - 5^b$	100 ± 20	135 ± 40	-80 ± 50	-140 ± 65	****	**
$N(1900)P_{13}$	$3/2^+$	1900 ± 30	200 ± 50	5 ± 2	24 ± 14	-67 ± 30	0 ± 30	-60 ± 45	***	**
$N(1700)D_{13}$	$3/2^-$	1700 ± 50	150^{+100}_{-50}	-	41 ± 17	-37 ± 14	25 ± 10	-32 ± 18	***	*
$N(1875)D_{13}$	$3/2^-$	1875^{+45}_{-55}	250 ± 70	seen	18 ± 10	-7 ± 4	10 ± 6	-20 ± 15	***	**
$N(2120)D_{13}$	$3/2^-$	2120 ± 45	340 ± 35	-	130 ± 50	160 ± 65	110 ± 45	40 ± 30	**	*
$N(2060)D_{15}$	$5/2^-$	2045 ± 15	420 ± 30	3 ± 2	62 ± 10	62 ± 20	25 ± 11	-37 ± 17	**	**
$N(2570)D_{15}$	$5/2^-$	2570^{+19+34}_{-10-10}	250^{+14+69}_{-24-21}	-	-	-	-	-	**	-
$N(1860)F_{15}$	$5/2^+$	1860^{+100}_{-40}	270^{+140}_{-50}	-	-17 ± 3	29 ± 4	21 ± 13	34 ± 17	**	-
$N(2000)F_{15}$	$5/2^+$	2060 ± 30	390 ± 55	-	31 ± 10	-43 ± 8	-18 ± 12	-35 ± 20	**	**
$N(1990)F_{17}$	$7/2^+$	2000^{+100}_{-50}	300 ± 100	-	40 ± 12	57 ± 12	-45 ± 20	-52 ± 27	**	*
$N(2190)G_{17}$	$7/2^-$	2190^{+10}_{-90}	500 ± 200	0.5 ± 0.3^b	-71 ± 6	27 ± 10	-15 ± 13	-34 ± 22	****	-
$N(2250)G_{19}$	$9/2^-$	2280^{+40}_{-30}	500^{+100}_{-200}	-	-	-	-	-	****	-
$N(2220)H_{19}$	$9/2^+$	2250 ± 50	400^{+100}_{-50}	-	-	-	-	-	****	-
$N(2600)I_{1,11}$	$11/2^-$	2600^{+150}_{-50}	650 ± 150	-	-	-	-	-	***	-
$N(2700)K_{1,13}$	$13/2^+$	2612 ± 45	350 ± 50	-	-	-	-	-	**	-

[a] Breit-Wigner definition.
[b] $K\Lambda$ decay mode. The $K\Sigma$ decay mode is not explicitly listed.

19 resonances

Delta Resonances Used in this Study

Table 3. Properties of the delta resonances used in the present work. The helicity amplitudes $A_{1/2}$ and $A_{3/2}$ are given in 10^{-3} GeV$^{-1/2}$ units. Data are taken from the Review of Particle Properties of Particle Data Group (PDG).[1]

State	J^P	M_R^a (MeV)	Γ_R^a (MeV)	β_K (%)	$A_{1/2}^a$	$A_{3/2}^a$	Overall status	Status in $K\Sigma$
$\Delta(1900)S_{31}$	$1/2^-$	1860^{+60}_{-20}	295 ± 30	seen	65 ± 15	-	**	**
$\Delta(1910)P_{31}$	$1/2^+$	1890^{+20}_{-30}	280 ± 60	9 ± 5	20 ± 10	-	****	*
$\Delta(1920)P_{33}$	$3/2^+$	1920^{+50}_{-20}	260^{+40}_{-80}	4 ± 2	130 ± 30	-105 ± 35	***	***
$\Delta(1700)D_{33}$	$3/2^-$	1700^{+50}_{-30}	300 ± 100	-	140 ± 30	140 ± 30	****	-
$\Delta(1940)D_{33}$	$3/2^-$	2000 ± 60	450 ± 70	-	170^{+110}_{80}	150 ± 80	**	-
$\Delta(1930)D_{35}$	$5/2^-$	1950 ± 50	360 ± 140	-	-7 ± 10	5 ± 10	***	-
$\Delta(1905)F_{35}$	$5/2^+$	1880^{+30}_{-25}	330^{+70}_{-60}	-	22 ± 5	-45 ± 10	****	***
$\Delta(2000)F_{35}$	$5/2^+$	2200 ± 125	400 ± 125	-	-61 ± 18	158 ± 32	**	-
$\Delta(1950)F_{37}$	$7/2^+$	1930^{+20}_{-15}	285 ± 50	0.4 ± 0.1	-67 ± 5	-94 ± 4	****	***
$\Delta(2400)G_{39}$	$9/2^-$	2643 ± 141	895 ± 432	-	-	-	**	-
$\Delta(2300)H_{39}$	$9/2^+$	2400 ± 125	425 ± 150	-	-	-	**	-
$\Delta(2420)H_{3,11}$	$11/2^+$	2420^{+80}_{-120}	400 ± 100	-	-	-	****	-
$\Delta(2750)I_{3,13}$	$13/2^-$	2794 ± 80	350 ± 100	-	-	-	**	-

[a]Breit-Wigner definition.

13 resonances

The Background Terms

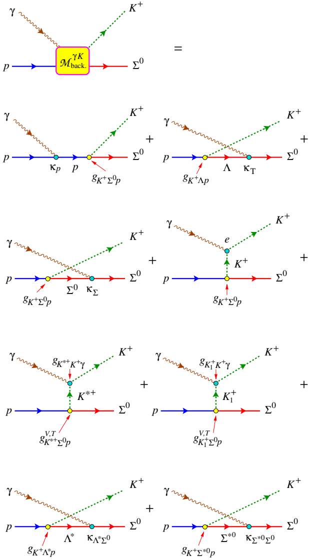

Decompose the background amplitude into

$$\mathcal{M}^{\gamma K}_{\rm back.} = \bar{u}_\Sigma \sum_{i=1}^{4} A_i(s,t,u)\, M_i\, u_N = \chi_{\rm f}^\dagger\; F\; \chi_{\rm i}\,,$$

with

$$\begin{aligned} M_1 &= \gamma_5\, \not\epsilon\, \not k\;, \\ M_2 &= 2\gamma_5\,(q\cdot\epsilon\; p\cdot k - q\cdot k\; p\cdot\epsilon)\;, \\ M_3 &= \gamma_5\,(q\cdot k\; \not\epsilon - q\cdot\epsilon\; \not k\,)\;, \\ M_4 &= i\,\epsilon_{\mu\nu\rho\sigma}\,\gamma^\mu\, q^\nu\, \epsilon^\rho\, k^\sigma\;, \end{aligned}$$

$$F = \sigma\cdot\epsilon\mathcal{F}_1 - i\sigma\cdot\hat{q}\;\sigma\cdot(\hat{k}\times\epsilon)\mathcal{F}_2 + \sigma\cdot\hat{k}\;\hat{q}\cdot\epsilon\mathcal{F}_3 + \sigma\cdot\hat{q}\;\hat{q}\cdot\epsilon\mathcal{F}_4\,.$$

$$\begin{aligned} \mathcal{F}_{1,2} &= \frac{1}{8\pi W}\left[(E_N\pm m_N)(E_\Sigma\pm m_\Sigma)\right]^{1/2}\Big[\pm(W\mp m_N)\,A_1 \\ &\quad + q\cdot k\,(A_3-A_4) + (W\mp m_N)(W\mp m_\Sigma)A_4\Big]\;, \\ \mathcal{F}_{3,4} &= \frac{|q|\,|k|}{8\pi W}\left(\frac{E_\Sigma\pm m_\Sigma}{E_N\pm m_N}\right)^{1/2}\Big[\pm(s-m_N^2)\,A_2 \\ &\quad + (W\pm m_N)\,(A_3-A_4)\Big]\,. \end{aligned}$$

Problem with the $K^0\Sigma^+$ and $K^+\Sigma^-$ Channels

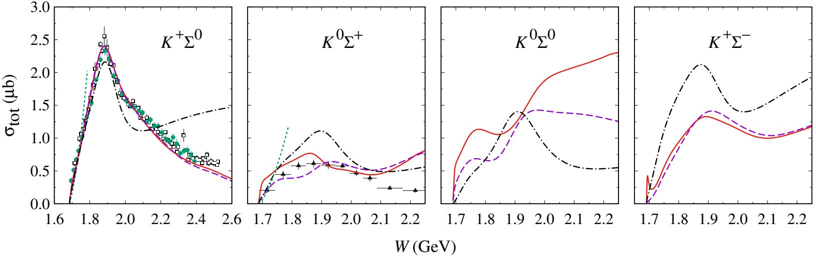

- The $K^0\Sigma^+$ data cannot be nicely reproduced
  - Needs a weighting factor
- A small spike near $K^+\Sigma^-$ channel $\rightarrow$ P_{11} state
  - Model 1 with P_{11} state
  - Model 2 without P_{11} state

Introduce a Weighting Factor

Instead of using

$$\chi^2 = \sum_{i=1}^{N} \left\{ \frac{\mathcal{O}_i^{\rm exp} - \mathcal{O}_i^{\rm th}}{\Delta \mathcal{O}_i^{\rm exp}} \right\}^2 ,$$

use Weighting Factor α,

$$\chi^2 = \sum_{i=1}^{N-N'} \left\{ \frac{\mathcal{O}_i^{\rm exp} - \mathcal{O}_i^{\rm th}}{\Delta \mathcal{O}_i^{\rm exp}} \right\}^2 + \alpha \sum_{j=1}^{N'} \left\{ \frac{\mathcal{O}_j^{\rm exp} - \mathcal{O}_j^{\rm th}}{\Delta \mathcal{O}_j^{\rm exp}} \right\}^2 , \quad (1)$$

with N' the number of $K^0\Sigma^+$ data and calculated only in the second summation.

But remember: α is unknown

Scan the Unknown Weighting Factor α

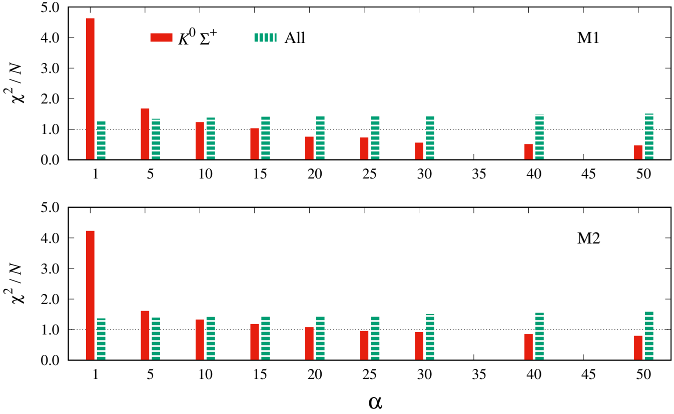

- Total χ^2 increases with increasing α
- $\alpha = 20$ is sufficient $\rightarrow$ $\chi^2(\mathrm{M1}) < 1.0$

With $\alpha = 20$

- M1 with $P_{11}(1710)$
- M2 without $P_{11}(1710)$
- Kaon-Maid Prediction

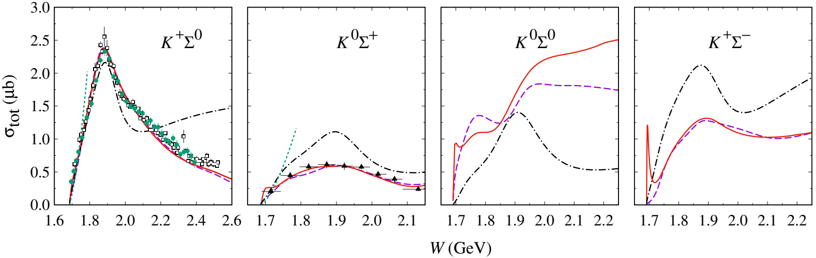

- All data are nicely reproduced
- Very sharp spike appears in $K^+\Sigma^-$ channel $\rightarrow$ Data??
- All K^0 channels show P_{11} peak at $W \approx 1710$ MeV

Properties of Nucleon Resonances Extracted from Fitting

Table 6. The extracted nucleon resonance parameters from fits to experimental data for the two different models (M1 and M2). The uncertainties in the extracted parameter values are merely obtained from MINUIT.[70] The units of helicity photon couplings $A_{1/2}$ and $A_{3/2}$ are given in 10^{-3} GeV$^{-1/2}$.

Resonance		M_R (MeV)	Γ_R (MeV)	β_K	ϕ (deg.)	$A_{1/2}(p)$	$A_{3/2}(p)$	$A_{1/2}(n)$	$A_{3/2}(n)$
$N(1895)S_{11}$	M1	1880 ± 0	170 ± 0	0.240 ± 0.001	231 ± 2	17 ± 0	-	21 ± 0	-
	M2	1880 ± 4	172 ± 3	0.240 ± 0.001	351 ± 1	17 ± 0	-	7 ± 0	-
$N(1710)P_{11}$	M1	1692 ± 0	125 ± 0	0.140 ± 0.000	265 ± 1	20 ± 0	-	-42 ± 11	-
	M2	-	-	-	-	-	-	0 ± 0	-
$N(1880)P_{11}$	M1	1910 ± 0	75 ± 2	0.100 ± 0.002	111 ± 3	12 ± 1	-	-4 ± 0	-
	M2	1880 ± 0	92 ± 4	0.100 ± 0.001	306 ± 1	18 ± 0	-	10 ± 1	-
$N(2300)P_{11}$	M1	2270 ± 1	252 ± 3	0.100 ± 0.004	133 ± 2	29 ± 1	-	35 ± 6	-
	M2	2363 ± 3	275 ± 7	0.100 ± 0.011	164 ± 1	35 ± 1	-	-22 ± 5	-
$N(1720)P_{13}$	M1	1705 ± 0	277 ± 6	0.002 ± 0.000	212 ± 1	120 ± 0	120 ± 0	22 ± 1	20 ± 32
	M2	1710 ± 0	150 ± 3	0.001 ± 0.000	227 ± 0	120 ± 1	120 ± 1	22 ± 2	-22 ± 9
$N(1900)P_{13}$	M1	1989 ± 4	186 ± 11	0.030 ± 0.000	264 ± 3	11 ± 0	-35 ± 0	-6 ± 1	-4 ± 1
	M2	1961 ± 3	150 ± 2	0.030 ± 0.000	299 ± 1	11 ± 0	-35 ± 0	-6 ± 2	-18 ± 2
$N(1700)D_{13}$	M1	1750 ± 0	123 ± 4	0.042 ± 0.002	360 ± 0	-4 ± 0	-35 ± 1	5 ± 0	-50 ± 0
	M2	1744 ± 0	100 ± 0	0.047 ± 0.001	360 ± 0	9 ± 0	-27 ± 0	5 ± 1	-50 ± 0
$N(1875)D_{13}$	M1	1820 ± 1	957 ± 15	0.011 ± 0.000	267 ± 3	28 ± 0	-14 ± 0	20 ± 16	-5 ± 2
	M2	1820 ± 0	957 ± 0	0.011 ± 0.000	239 ± 1	28 ± 0	-14 ± 0	20 ± 2	-9 ± 3
$N(2120)D_{13}$	M1	2114 ± 4	375 ± 1	0.015 ± 0.001	53 ± 1	83 ± 4	179 ± 9	39 ± 4	20 ± 5
	M2	2112 ± 3	375 ± 2	0.005 ± 0.000	36 ± 1	80 ± 0	210 ± 1	-65 ± 9	20 ± 2
$N(2060)D_{15}$	M1	2160 ± 0	350 ± 1	0.022 ± 0.001	203 ± 2	77 ± 0	26 ± 2	2 ± 7	-0 ± 1
	M2	2160 ± 1	350 ± 1	0.042 ± 0.001	254 ± 0	53 ± 0	70 ± 1	5 ± 3	-0 ± 2
$N(2570)D_{15}$	M1	2550 ± 1	333 ± 0	0.099 ± 0.001	360 ± 0	44 ± 1	-6 ± 1	-51 ± 21	-165 ± 16
	M2	2550 ± 1	333 ± 1	0.100 ± 0.016	360 ± 0	52 ± 1	-9 ± 1	39 ± 4	-16 ± 11
$N(1860)F_{15}$	M1	1820 ± 2	410 ± 2	0.003 ± 0.000	166 ± 1	8 ± 0	70 ± 0	5 ± 1	-4 ± 2
	M2	1960 ± 3	307 ± 4	0.100 ± 0.012	27 ± 0	32 ± 3	53 ± 0	15 ± 7	-14 ± 1
$N(2000)F_{15}$	M1	2066 ± 5	300 ± 5	0.033 ± 0.002	360 ± 1	20 ± 1	64 ± 1	30 ± 4	-24 ± 8
	M2	1950 ± 1	192 ± 3	0.100 ± 0.004	208 ± 0	22 ± 0	46 ± 0	11 ± 2	20 ± 1
$N(1990)F_{17}$	M1	2090 ± 0	290 ± 2	0.004 ± 0.000	271 ± 3	39 ± 4	70 ± 2	-10 ± 13	-168 ± 4
	M2	1932 ± 4	290 ± 13	0.003 ± 0.000	194 ± 1	56 ± 0	70 ± 1	10 ± 3	-168 ± 1
$N(2190)G_{17}$	M1	2114 ± 6	300 ± 3	0.015 ± 0.001	183 ± 2	-57 ± 1	21 ± 2	-36 ± 9	20 ± 5
	M2	2100 ± 6	428 ± 14	0.006 ± 0.000	212 ± 1	-73 ± 1	18 ± 0	-65 ± 4	20 ± 2
$N(2250)G_{19}$	M1	2200 ± 1	800 ± 6	0.100 ± 0.001	30 ± 3	20 ± 0	20 ± 0	33 ± 5	-45 ± 5
	M2	2261 ± 4	230 ± 2	0.100 ± 0.066	79 ± 3	20 ± 2	0 ± 0	4 ± 3	17 ± 3
$N(2220)H_{19}$	M1	2200 ± 1	500 ± 5	0.100 ± 0.001	152 ± 3	10 ± 0	0 ± 1	23 ± 3	-16 ± 5
	M2	2200 ± 2	500 ± 5	0.100 ± 0.062	141 ± 2	3 ± 0	0 ± 0	15 ± 2	-63 ± 2
$N(2600)I_{1,11}$	M1	2550 ± 2	500 ± 3	0.100 ± 0.001	329 ± 4	14 ± 1	10 ± 1	29 ± 24	-30 ± 21
	M2	2713 ± 10	500 ± 5	0.100 ± 0.079	239 ± 3	-15 ± 1	2 ± 1	-65 ± 84	6 ± 17
$N(2700)K_{1,13}$	M1	2800 ± 2	400 ± 8	0.043 ± 0.013	275 ± 2	20 ± 3	-1 ± 2	7 ± 65	-178 ± 138
	M2	2800 ± 1	400 ± 10	0.062 ± 0.003	235 ± 1	18 ± 0	-6 ± 1	39 ± 17	-178 ± 198

within the PDG error bars

Properties of Delta Resonances Extracted from Fitting

Table 7. As in Table 6, but for the delta resonances extracted from both models (M1 and M2).

Resonance		M_R (MeV)	Γ_R (MeV)	β_K	ϕ (deg.)	$A_{1/2}$	$A_{3/2}$
$\Delta(1900)S_{31}$	M1	1866 ± 2	255 ± 0	0.088 ± 0.002	80 ± 1	75 ± 0	0 ± 0
	M2	1859 ± 1	255 ± 0	0.100 ± 0.000	68 ± 0	75 ± 0	0 ± 0
$\Delta(1910)P_{31}$	M1	1860 ± 0	340 ± 1	0.130 ± 0.001	206 ± 1	30 ± 0	0 ± 0
	M2	1860 ± 0	340 ± 1	0.130 ± 0.011	122 ± 1	26 ± 0	0 ± 0
$\Delta(1920)P_{33}$	M1	1913 ± 2	180 ± 0	0.018 ± 0.000	26 ± 1	70 ± 0	-90 ± 0
	M2	1920 ± 1	180 ± 1	0.018 ± 0.000	41 ± 0	70 ± 0	-96 ± 1
$\Delta(1700)D_{33}$	M1	1694 ± 0	400 ± 2	0.000 ± 0.000	140 ± 2	170 ± 0	110 ± 0
	M2	1703 ± 0	385 ± 18	0.000 ± 0.000	148 ± 1	170 ± 1	110 ± 1
$\Delta(1940)D_{33}$	M1	1940 ± 0	350 ± 5	0.100 ± 0.001	275 ± 1	21 ± 1	-28 ± 1
	M2	1940 ± 1	350 ± 1	0.100 ± 0.002	334 ± 0	22 ± 3	-24 ± 0
$\Delta(1930)D_{35}$	M1	2000 ± 0	220 ± 7	0.052 ± 0.002	167 ± 1	-37 ± 1	-24 ± 1
	M2	1946 ± 1	220 ± 0	0.100 ± 0.001	153 ± 0	-37 ± 0	-17 ± 0
$\Delta(1905)F_{35}$	M1	1855 ± 2	400 ± 9	0.007 ± 0.001	337 ± 2	19 ± 1	-35 ± 1
	M2	1855 ± 1	400 ± 4	0.003 ± 0.000	191 ± 1	27 ± 0	-35 ± 0
$\Delta(2000)F_{35}$	M1	1983 ± 3	98 ± 9	0.000 ± 0.000	360 ± 0	-43 ± 6	190 ± 7
	M2	2100 ± 3	206 ± 1	0.001 ± 0.000	202 ± 1	-43 ± 1	190 ± 4
$\Delta(1950)F_{37}$	M1	1950 ± 0	235 ± 2	0.003 ± 0.000	162 ± 2	-64 ± 0	-87 ± 0
	M2	1950 ± 0	235 ± 1	0.003 ± 0.000	360 ± 0	-64 ± 0	-87 ± 0
$\Delta(2400)G_{39}$	M1	2440 ± 8	663 ± 2	0.100 ± 0.001	28 ± 2	28 ± 1	37 ± 1
	M2	2422 ± 7	663 ± 8	0.100 ± 0.065	63 ± 1	17 ± 1	68 ± 1
$\Delta(2300)H_{39}$	M1	2200 ± 3	33 ± 1	0.000 ± 0.000	127 ± 7	72 ± 17	95 ± 20
	M2	2400 ± 5	33 ± 2	0.000 ± 0.000	191 ± 11	161 ± 34	103 ± 37
$\Delta(2420)H_{3,11}$	M1	2472 ± 7	300 ± 2	0.001 ± 0.000	341 ± 3	134 ± 10	113 ± 9
	M2	2368 ± 8	300 ± 3	0.000 ± 0.000	232 ± 3	208 ± 11	73 ± 11
$\Delta(2750)I_{3,13}$	M1	2826 ± 12	250 ± 18	0.002 ± 0.001	0 ± 5	36 ± 7	-8 ± 2
	M2	2650 ± 1	450 ± 3	0.100 ± 0.073	262 ± 2	7 ± 0	5 ± 0

within the PDG error bars

Results for the $K^+\Sigma^0$ Differential Cross Section and Recoil Polarization

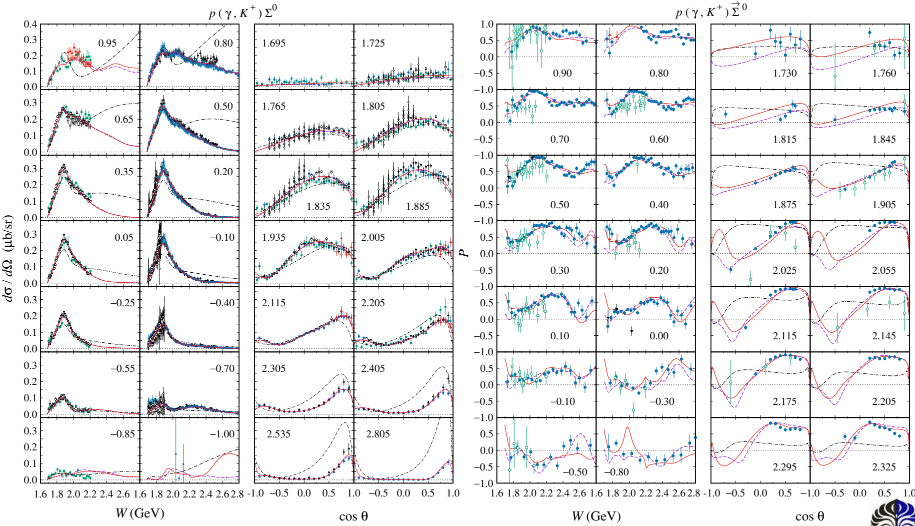

Results for the $K^0\Sigma^+$ and $K^+\Sigma^-$ Channels

- For the $K^0\Sigma^+$ the bump is still within the data error bars
- For the $K^+\Sigma^-$ no data near the spikes at $W \approx 1710$ MeV

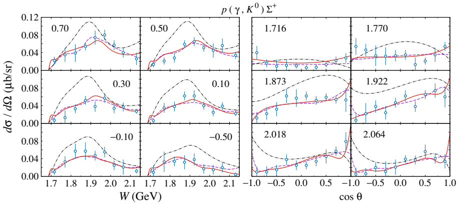

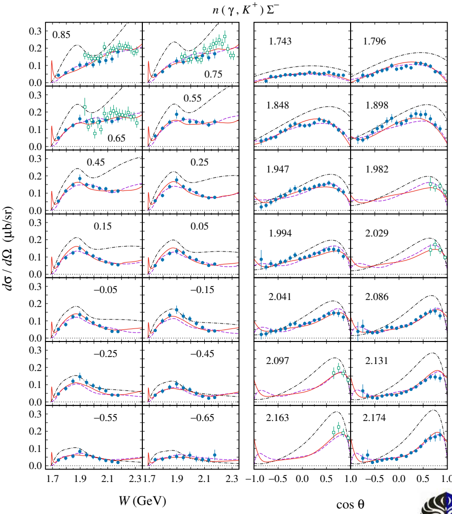

The $N(1535)S_{11}$ coupling strength to the $K\Sigma$ channel

The $N(1535)S_{11}$ is of special interest due to large branching to ηN channel (32−52%) and the so-called mass reverse problem: quark model predicts it to be the lowest mass nucleon resonance, but PDG puts $N(1440)P_{11}$.

Solution: $K\Lambda$-$K\Sigma$ & meson-baryon quasi-bound states, meson cloud effect, and pentaquark component in nucleon $\rightarrow$ large $g_{N(1535)\Lambda K^+}$ coupling.

- $J/\psi \rightarrow \bar{p}K^+\Lambda$ and $J/\psi \rightarrow \bar{p}p\eta$ data Liu and Zou [PRL **96** (2006) 042002]:

$$R_\Lambda \equiv \left| \frac{g_{N(1535)\Lambda K^+}}{g_{N(1535)\eta p}} \right| = 1.3 \pm 0.3$$

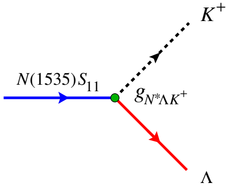

- TM, PRC **87** (2013) 042201: $R_\Lambda = 0.460 \pm 0.172$
- Partial wave: $R_\Lambda = 0.5 \sim 0.7^\dagger$
- Coupled-channels: $R_\Lambda = 0.8 \sim 2.6^\ddagger$

What about R_Σ ???

†, ‡ for references see TM, PRC**87** (2013) 042201

The $N(1535)S_{11}$ coupling strength to the $K\Sigma$ channel

- Insert the $N(1535)S_{11}$ exchange in the model
- Extract the $G_{N^*} \equiv g_{\gamma pN^*}\, g_{N^*\Sigma^0 K^+}$ values from the fits
- Use $A^p_{1/2}$ from PDG and

$$A^p_{1/2} = \frac{1}{2m_p}\left(\frac{m^2_{N^*}-m^2_p}{2m_p}\right)^{1/2} e g_{\gamma pN^*}$$

determine $g_{\gamma pN^*}$

- Use $g_{N^*(1535)\eta p} = 1.853 \pm 0.244$†

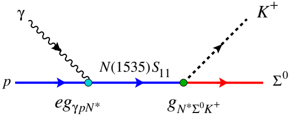

Parameter	M1	M2
$g_{\gamma pN^*}\, g_{N^*\Sigma^0K^+}$	-0.352 ± 0.013	0.061 ± 0.011
$g_{\gamma pN^*}$	0.428 ± 0.056	0.428 ± 0.056
$g_{N^*\Sigma^0K^+}$	-0.821 ± 0.111	0.142 ± 0.032
$g_{N^*(1535)\eta p}$	1.853 ± 0.244	1.853 ± 0.244
R_Σ	0.443 ± 0.084	0.077 ± 0.020
$\Delta\chi^2/N_{\rm dof}$	0.06	0.01

We obtain small $R_\Sigma \equiv \left|\frac{g_{N(1535)\Sigma^0K^+}}{g_{N(1535)\eta p}}\right|$

M1 : 0.443 ± 0.084 M2 : 0.077 ± 0.020

† see TM, PRC**87** (2013) 042201

Contribution of the $K\Sigma$ Channels to the Gerasimov-Drell-Hearn sum rule

The Gerasimov-Drell-Hearn (GDH) sum rule relates the static property of nucleon (anomalous magnetic moment of the nucleon κ_N) to its excited property (polarized total photoabsorption cross sections), i.e.,

$$\kappa_N^2 = \frac{m_N^2}{2\pi^2\alpha}\int_{E_\gamma^{\rm thr}}^{\infty}\frac{dE_\gamma}{E_\gamma}\left\{\sigma_{3/2}(E_\gamma)-\sigma_{1/2}(E_\gamma)\right\} .$$

For the proton, if we define

$$I_{\rm GDH} \equiv \int_{E_\gamma^{\rm thr}}^{\infty}\frac{dE_\gamma}{E_\gamma}\left[\sigma_{1/2}(E_\gamma)-\sigma_{3/2}(E_\gamma)\right]$$

$$= -\frac{2\pi^2\alpha\kappa^2}{m_p^2} = -204.5\ \mu\text{b}.$$

Meanwhile $\sigma_{\rm TT'} = (\sigma_{3/2}-\sigma_{1/2})/2$ and therefore

$$I_{\rm GDH} = \int_{E_\gamma^{\rm thr}}^{\infty} dE_\gamma\left\{-\frac{2\sigma_{\rm TT'}(E_\gamma)}{E_\gamma}\right\} .$$

can be calculated for individual contributions.

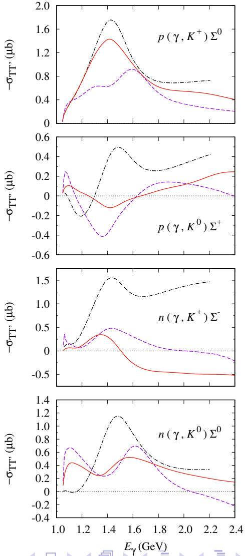

Contribution of the $K\Sigma$ Channels to the Gerasimov-Drell-Hearn sum rule

Channel	Kaon-Maid	M1	M2
proton:			
$\gamma + p \to K^+ + \Sigma^0$	1.38	1.15	0.95
$\gamma + p \to K^0 + \Sigma^+$	0.30	0.24	0.07
total	1.68	1.39	1.02
neutron:			
$\gamma + n \to K^+ + \Sigma^-$	1.55	-0.42	0.34
$\gamma + n \to K^0 + \Sigma^0$	0.72	0.85	1.03
total	2.27	0.43	1.37

sizable contributions!!

Other Applications

- Hypernuclear photo- and electroproduction

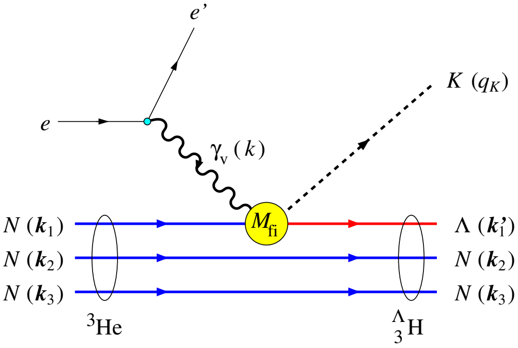

Conclusion

- We have analyzed $K\Sigma$ photoproduction near threshold and at energies above threshold up to $W = 2.8$ GeV.
- The multipole model yields a good agreement between data and calculated observables.
- A number of applications are in order.
- Contribution of individual resonances will be investigated in the future.

THANK YOU FOR YOUR PATIENCE